Electronic Supplementary Information for

Amethyrin-type expanded porphyrins that displays anti-aromatic character upon protonation

Harrison D. Root, [†] Daniel N. Mangel, [†] James T. Brewster II, [†] Hadiqa Zafar, Adam Samia, Graeme Henkelman,* and Jonathan L. Sessler*

Department of Chemistry, The University of Texas at Austin, Texas 78712-1224, USA

sessler@cm.utexas.edu; henkelman@utexas.edu

Contents

General materials and methods

All reagents and solvents were purchased from commercial suppliers and used without further purification. Proton NMR spectra were recorded using a Varian 400 spectrometer at room temperature. Chemical shifts are reported in ppm using TMS or solvent residual signals as internal reference standards. All NMR spectroscopic solvents were purchased from Cambridge Isotope Laboratories. UV-Vis spectra were recorded from 250 to 800 nm using a Varian Cary 5000 spectrophotometer at room temperature. A cell length of 10 mm was used for all UV-Vis spectral studies. Macrocycles were synthesized according to literature procedures.[1–3]

UV-Vis spectroscopic titrations

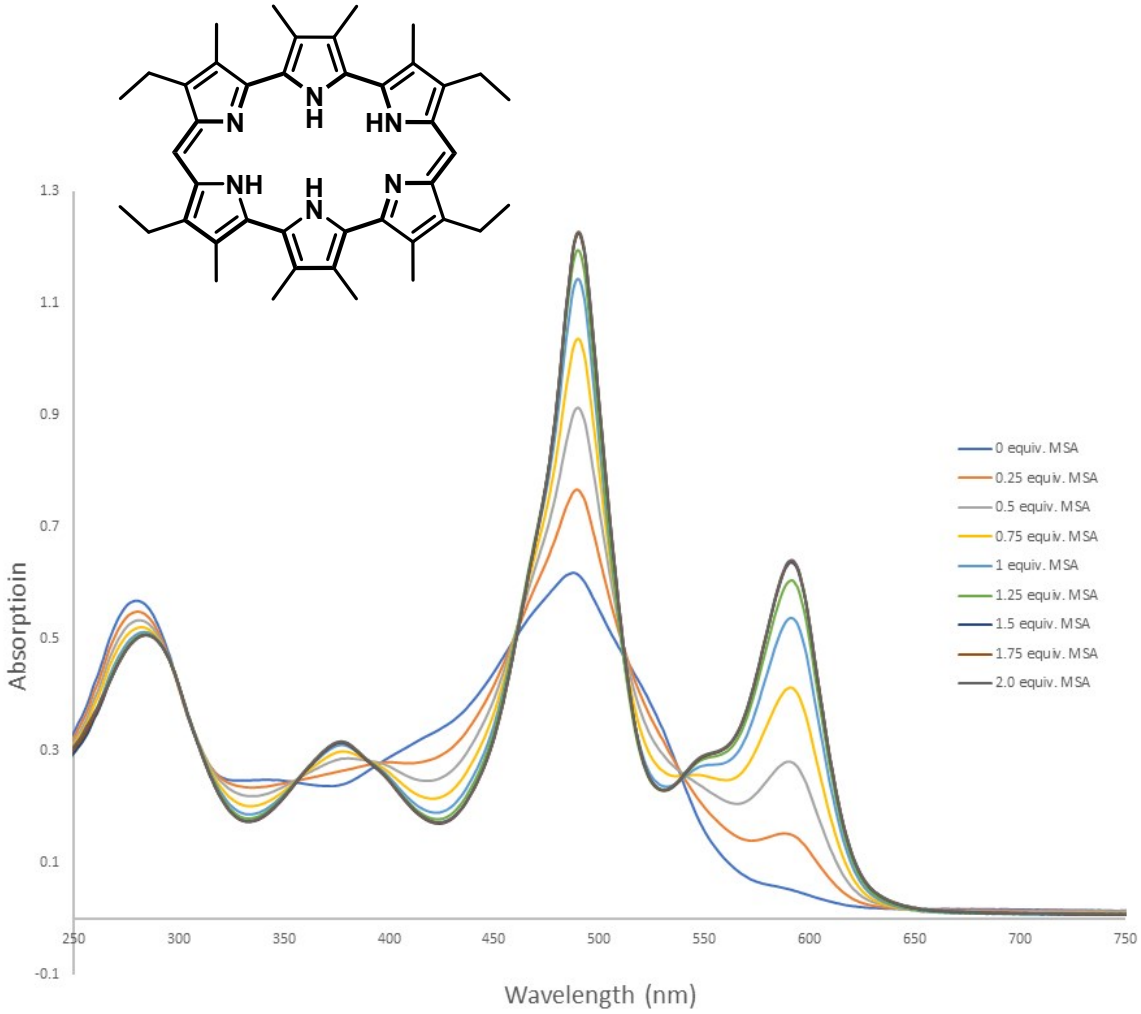

Figure S1. UV-Vis spectroscopic titration of amethyrin (**2**) with MSA in chloroform. The appearance of new Q-type bands and an increase in signal intensity was taken as evidence of increased π-conjugation.

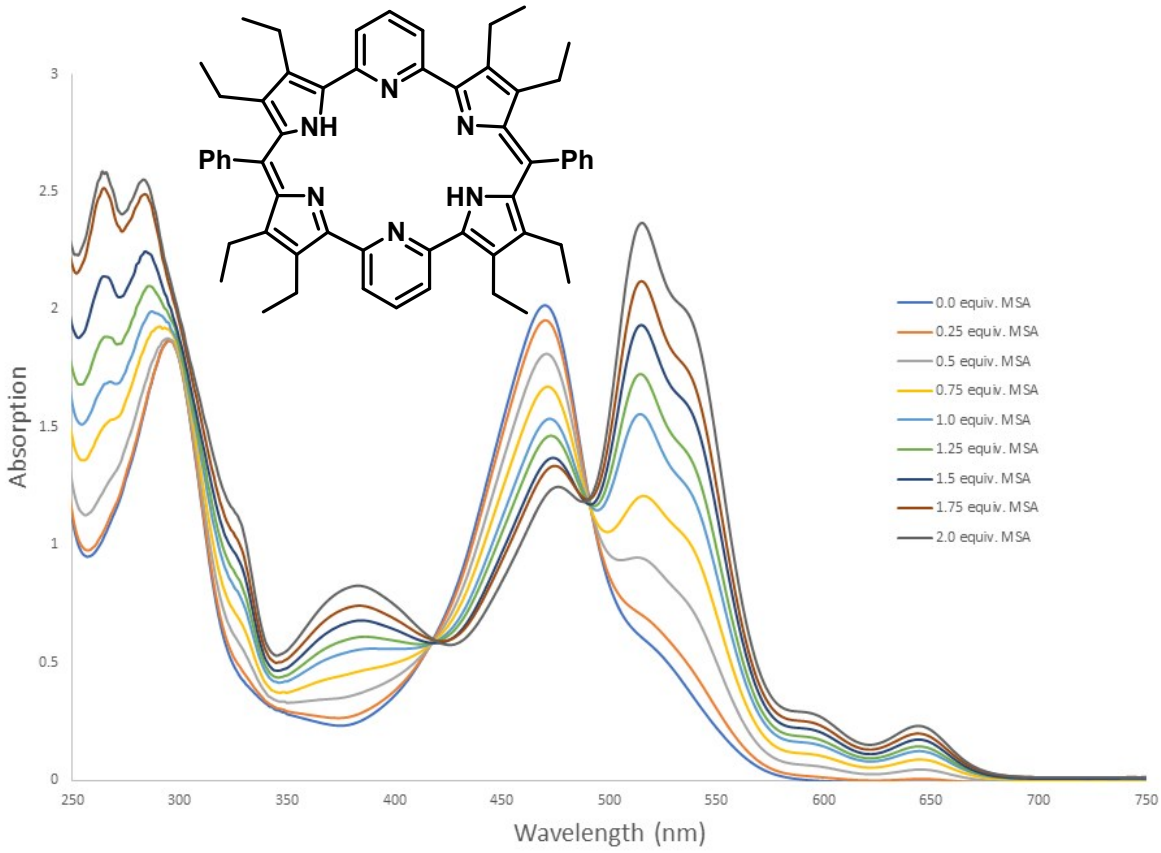

Figure S2. UV-Vis titration of dipyriamethyrin (**4**) with MSA in chloroform. The red shift in the Soret-like band and appearance of Q-type bands was taken as evidence of increased π-conjugation.

NMR spectroscopic titrations with MSA-d_4

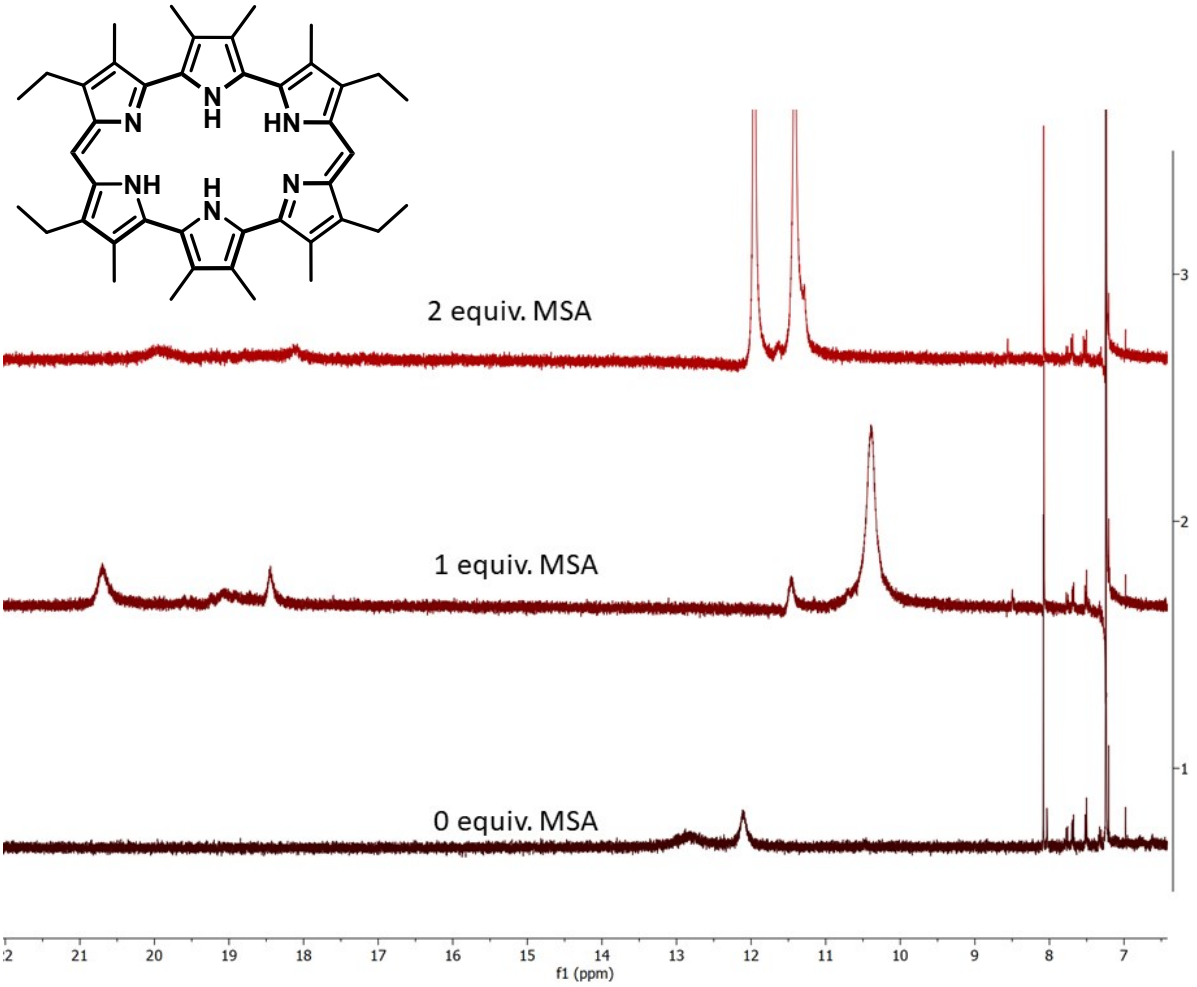

Figure S3. NMR spectroscopic titration of amethyrin (**2**) with MSA-d_4. Downfield shifts in the pyrrole N*H* resonances was taken as evidence of increased anti-aromatic character.

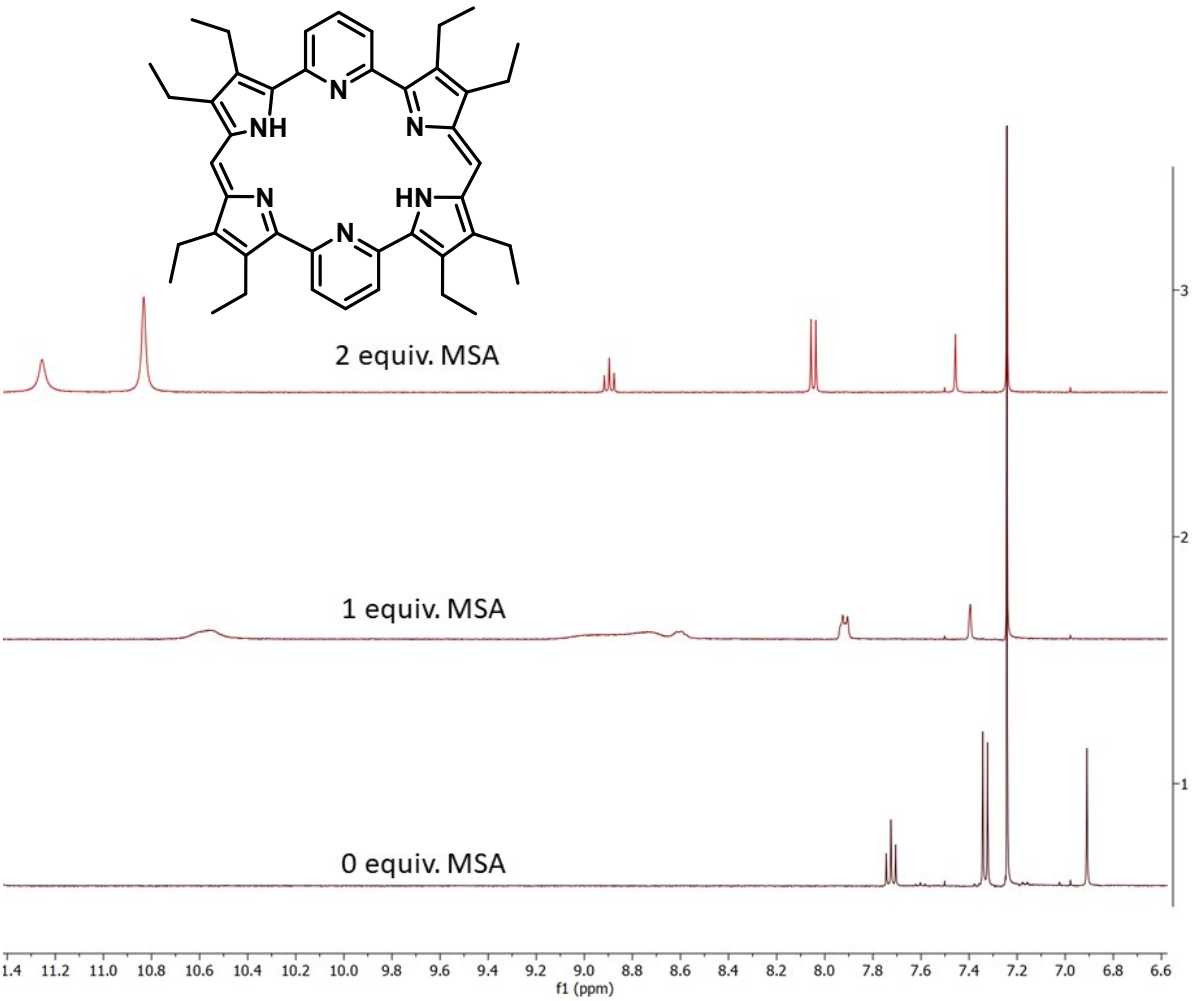

Figure S4. NMR titration of dipyriamethyrin (**3**) with MSA-d_4. Downfield shifts in the pyrrole N*H* resonances were taken as evidence of increased anti-aromatic character.

Calculations

Theoretical calculations were performed with the Gaussian16 program suite using the Texas Advanced Computing Center's (TACC) Stampede2 supercomputer. Calculations were carried out using the density functional theory (DFT) method with Becke's three-parameter hybrid exchange functionals and the Lee-Yang-Parr correlation functional (B3LYP) employing the 6-31G+(d) basis set. It is important to note that while accurately predicting the electronic nature, the B3LYP functional has been shown to overestimate paratropic properties in porphyrinoids, and thus the magnitude of the values should not be considered *per se*, but in the context of a comparison between the different complexes.[4] All calculations were performed using the Gaussian 16 software package unless otherwise specified. Geometry optimizations were carried out based on the crystal structures and the nature of the extrema was verified with analytical frequency calculations. No symmetry constraints were imposed. To simulate the steady-state absorption spectra, the time-dependent (TD)-DFT calculations were employed at the B3LYP/6-31+G(d) level. Anisotropy of the current-induced density (ACID) plots were obtained employing a continuous set of gauge transformations (CSGT) to calculate the current densities, and the results were plotted using POVRAY 3.7 on a Linux system. The ACID 3.0.1 software package obtained directly from Professor Herges' research group, whom we thank for making these materials available. Gauge including magnetically induced current density calculations were performed using the GIMIC version 2.0 software package as obtained through their GitHub database (https://github.com/qmcurrents/gimic). Integrated current densities were calculated using constant plane perpendicular to the bonds. Harmonic oscillator model for aromaticity (HOMA) analyses were performed using the Multiwfn program version 3.6. Integrated current densities through selected bonds were derived using the gauge-including magnetic induced current (GIMIC) method paired with the Gaussian 16 software package. The integration of the current density through a bond was performed using a rectangular plane perpendicular to the plane of the macrocycle. The rectangular plane had dimensions of 12 Å high 4 Å wide and spanned the center of the bond of interest, and was set so as to avoid all uninvolved atoms. The magnetic field was placed perpendicular to the plane of the macrocycle.

HOMA

The harmonic oscillator model of aromaticity (HOMA) has long been used as an index of aromaticity.[5] HOMA values were calculated for compounds 1-3 using X-ray crystal data and optimized structures for the protonated species 1b-3b. The HOMA value calculated for 1, calculated using an available X-ray structure, showed a HOMA value of 0.053, indicating little (anti)aromaticity throughout the macrocycle. Upon protonation, macrocycle 1b was characterized by a HOMA value of 0.731, signifying an increase in global conjugation and anti-aromaticity. HOMA calculations for 3 and 3b were also consistent with an increase in global anti-aromaticity, with the HOMA values increasing from 0.476 in the free-base form (3) to 0.725 in the protonated form (3b).

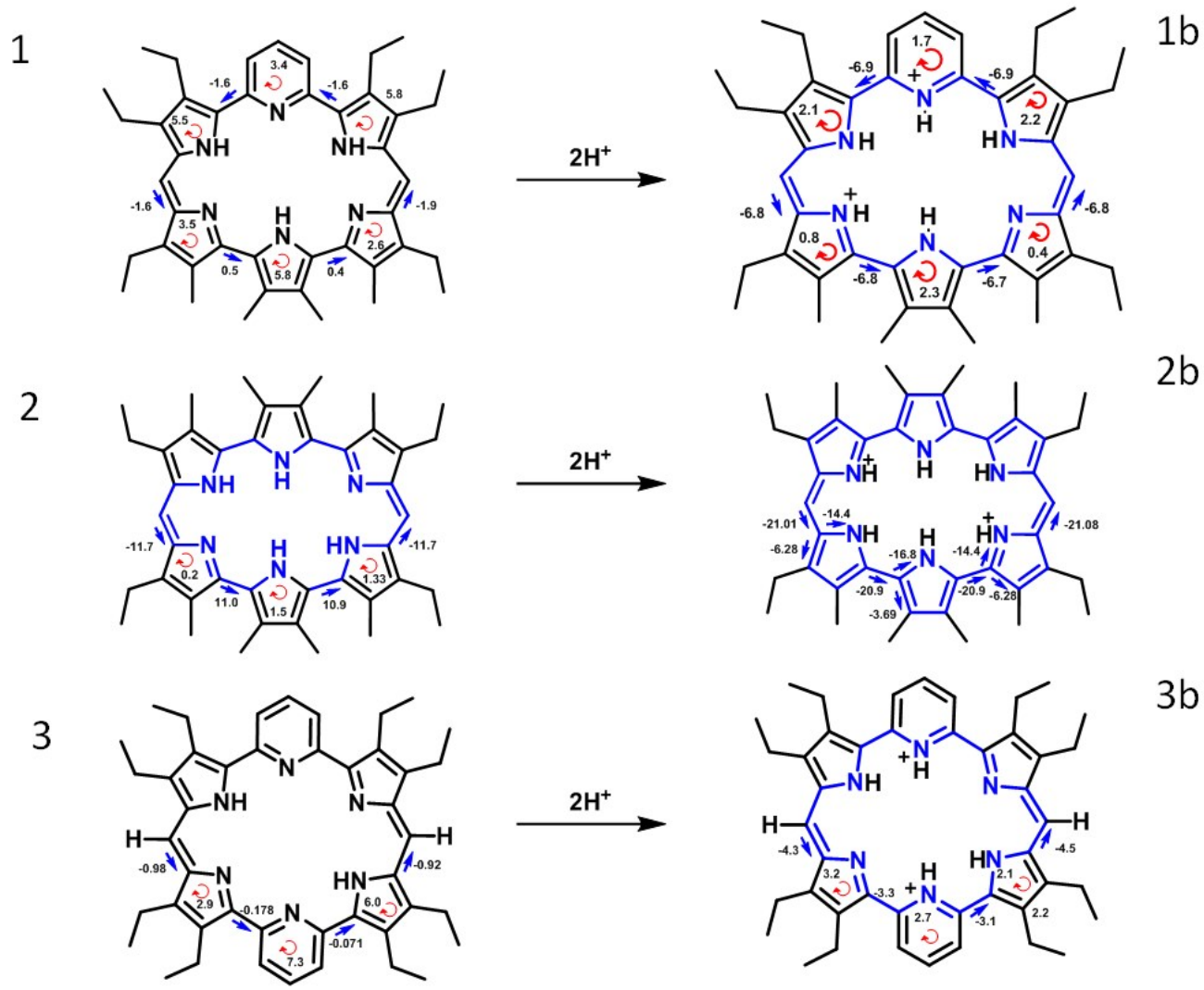

Figure S5. Integrated current densities through selected bonds as derived using the gauge including magnetic induced current (GIMIC) method paired with the Gaussian 16 software package.

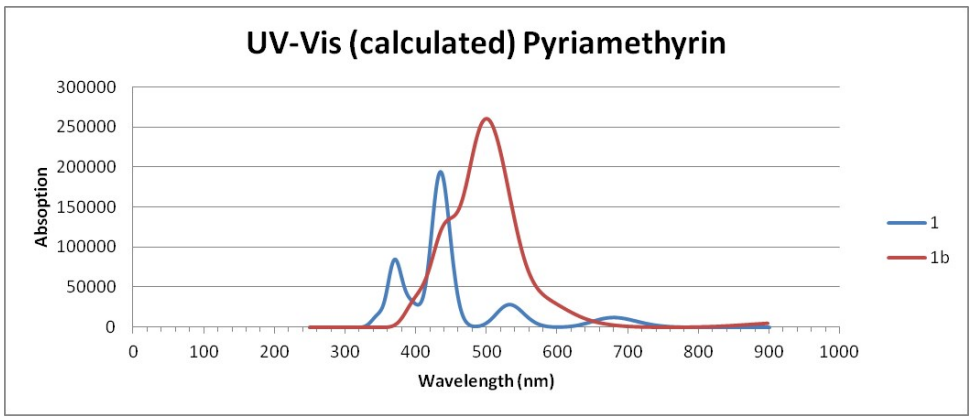

Figure S6. Calculated UV-VIS spectra of neutral and diprotonated pyriamethyrin (**1** and **1b**). TD-DFT calculations were performed at the B3LYP/6-31+G(d) level.

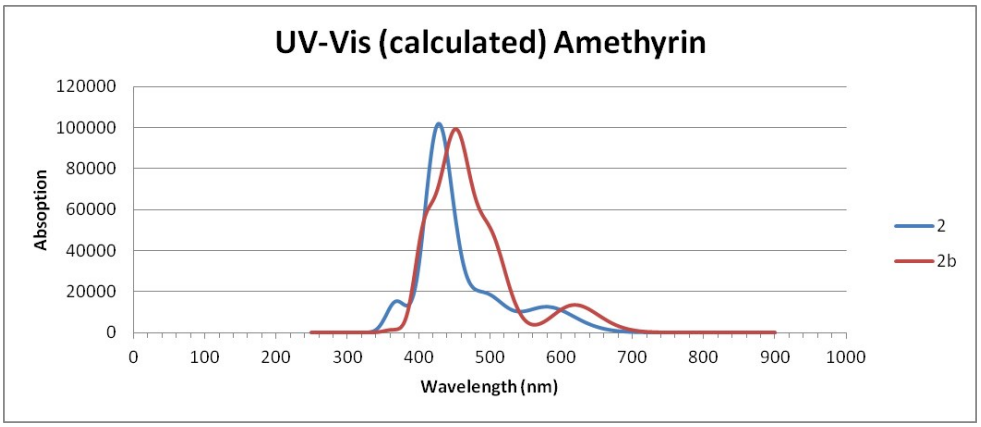

Figure S7. Calculated UV-VIS spectra of neutral and diprotonated amethyrin (**2** and **2b**). TD-DFT calculations were performed at the B3LYP/6-31+G(d) level.

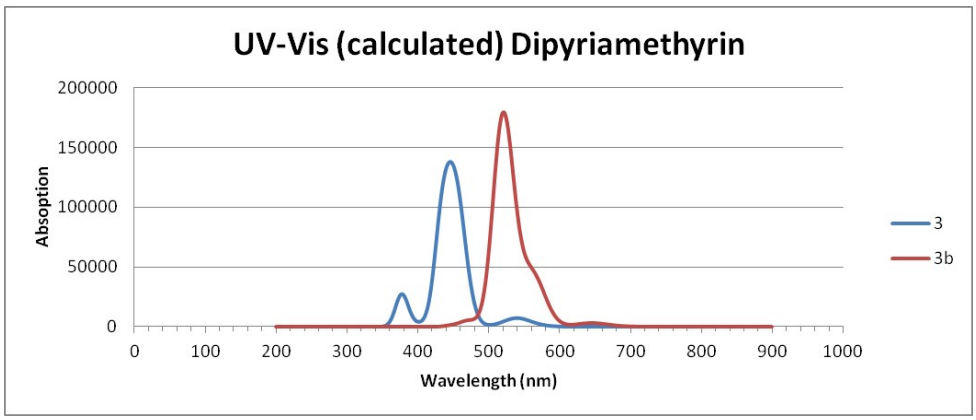

Figure S8. Calculated UV-VIS spectra of neutral and diprotonated dipyriamethyrin (**3** and **3b**). TD-DFT calculations were performed at the B3LYP/6-31+G(d) level.

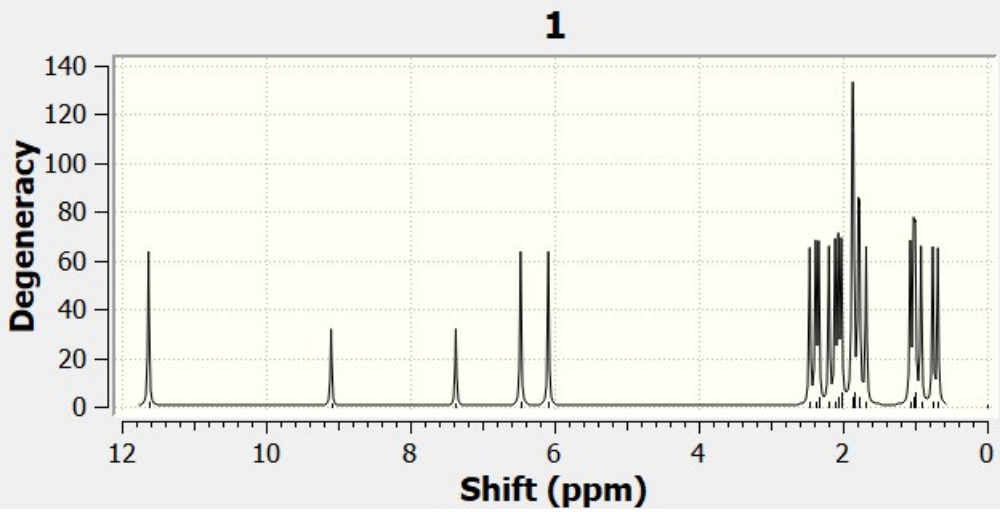

Figure S9. Calculated ^{1}H NMR spectra of pyriamethyrin **1**. The NMR shielding tensors were predicted using the continuous set of gauge transformations (CSGT) method at the B3LYP/6-31+G(d) level.

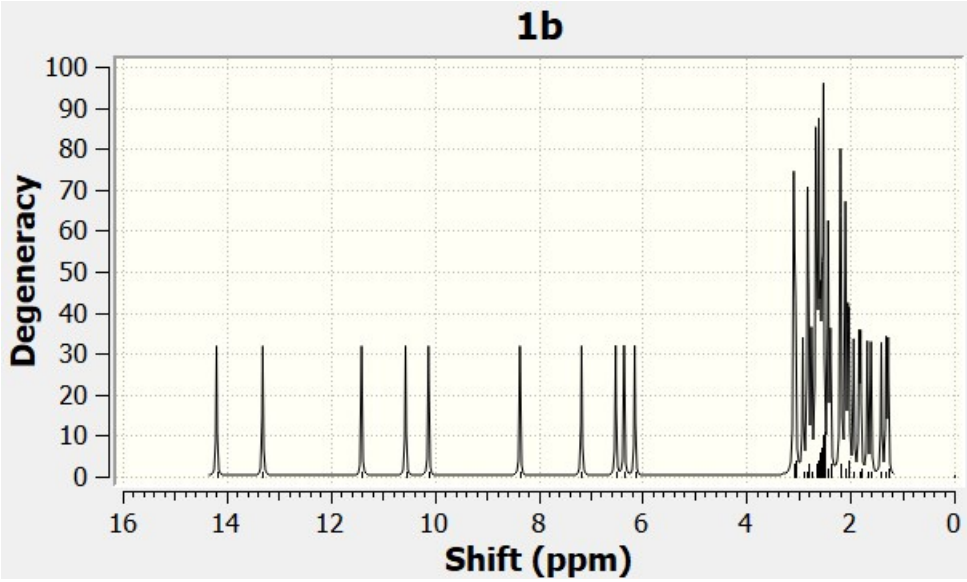

Figure S10. Calculated ^{1}H NMR spectra of diprotonated pyriamethyrin **1b**. The NMR shielding tensors were predicted using the continuous set of gauge transformations (CSGT) method at the B3LYP/6-31+G(d) level.

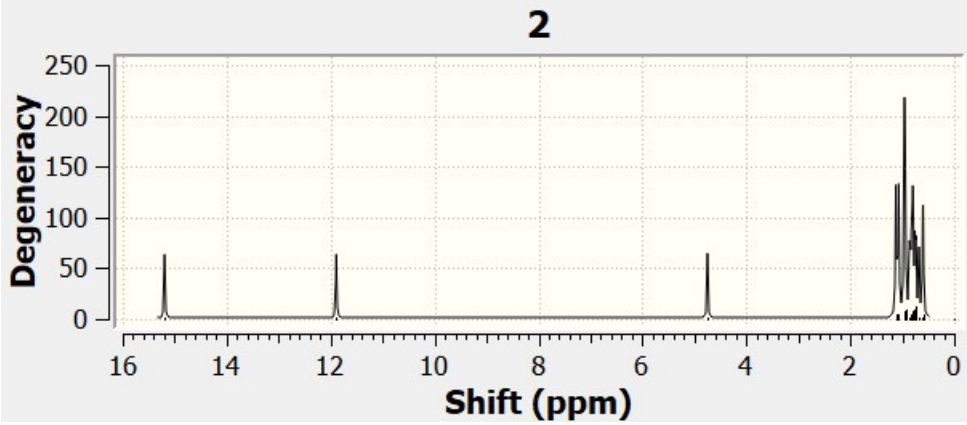

Figure S11. Calculated ^{1}H NMR spectra of amethyrin **2**. The NMR shielding tensors were predicted using the continuous set of gauge transformations (CSGT) method at the B3LYP/6-31+G(d) level.

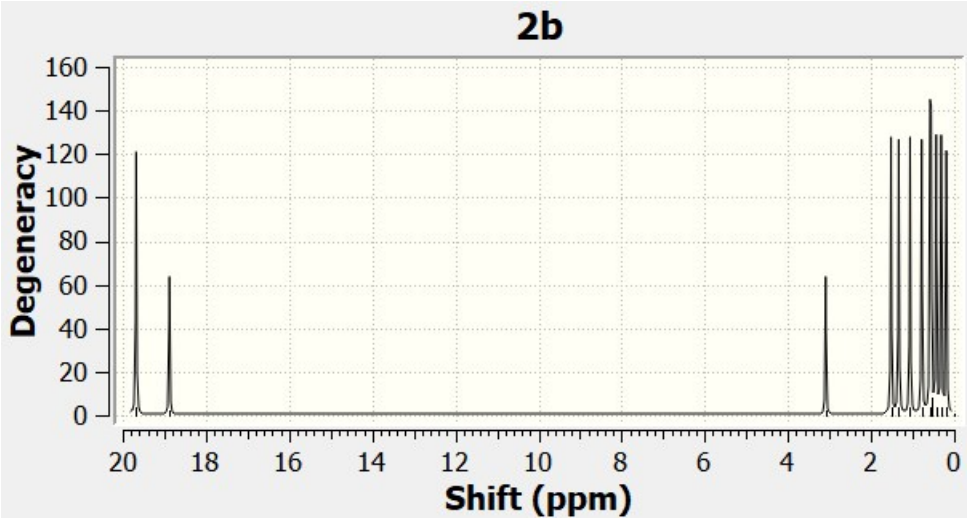

Figure S12. Calculated ^{1}H NMR spectra of diprotonated amethyrin **2b**. The NMR shielding tensors were predicted using the continuous set of gauge transformations (CSGT) method at the B3LYP/6-31+G(d) level.

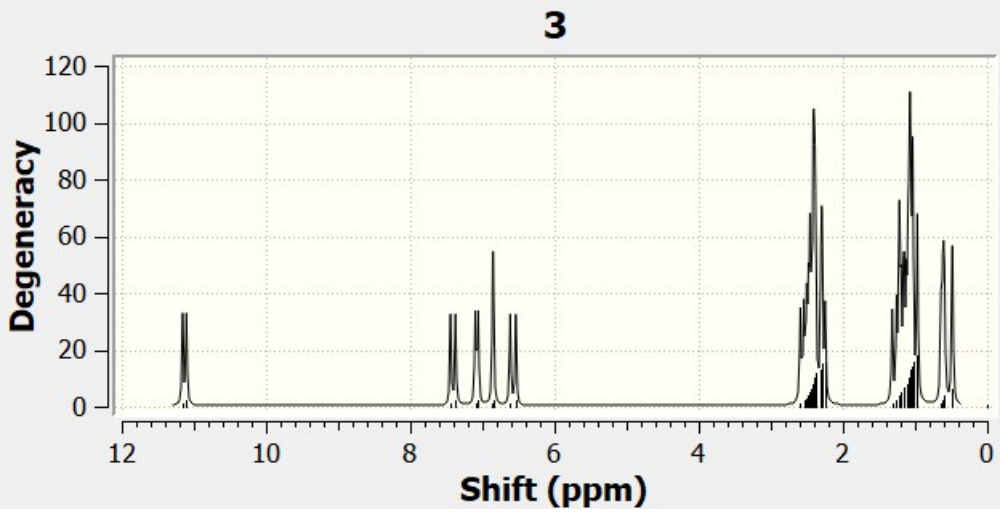

Figure S13. Calculated ^{1}H NMR spectra of dipyriamethyrin **3**. The NMR shielding tensors were predicted using the continuous set of gauge transformations (CSGT) method at the B3LYP/6-31+G(d) level.

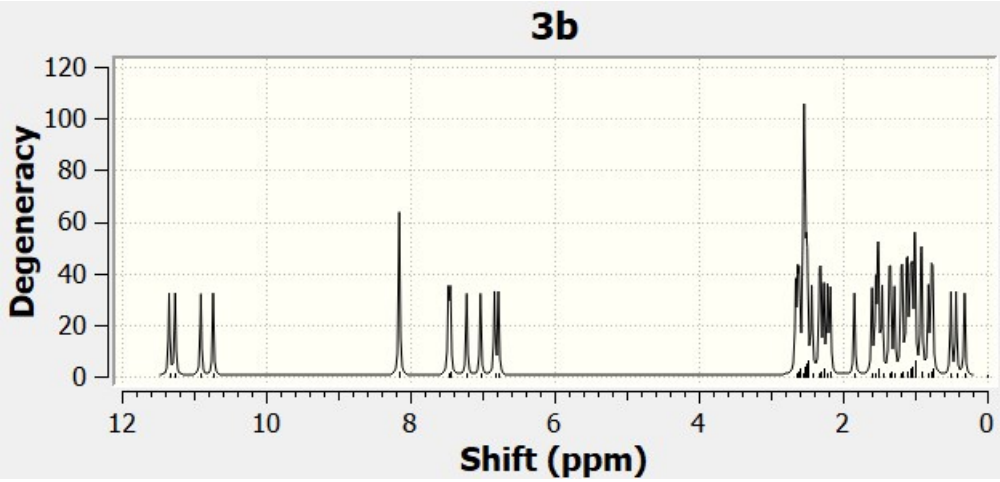

Figure S14. Calculated ^{1}H NMR spectra of diprotonated dipyriamethyrin **3b**. The NMR shielding tensors were predicted using the continuous set of gauge transformations (CSGT) method at the B3LYP/6-31+G(d) level.

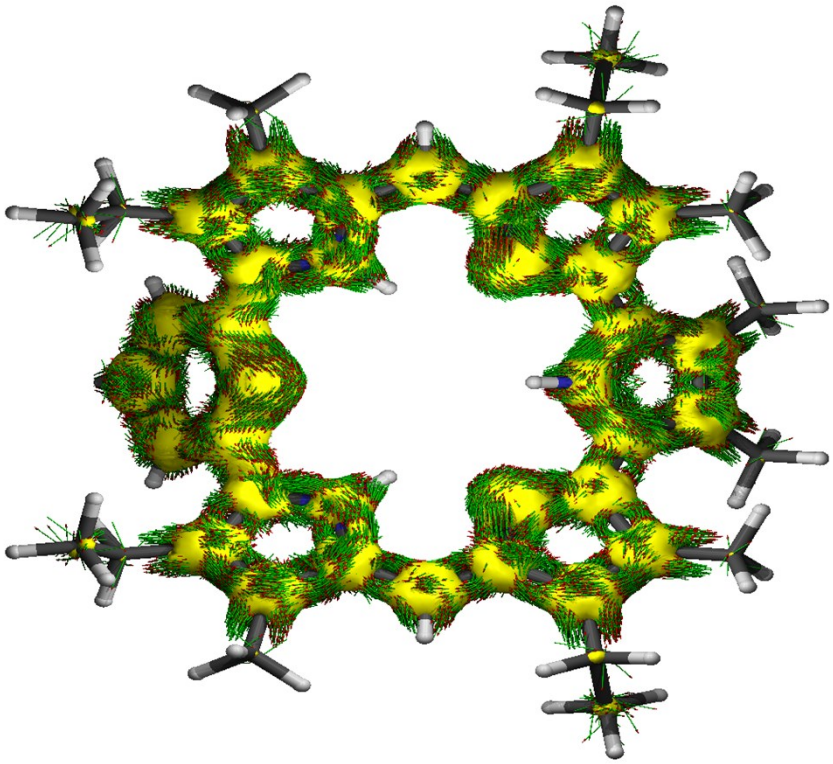

Figure S15. Calculated anisotropy induced current density (ACID) plot of pyriamethyrin **1**. Current density vectors indicate little global current directionality.

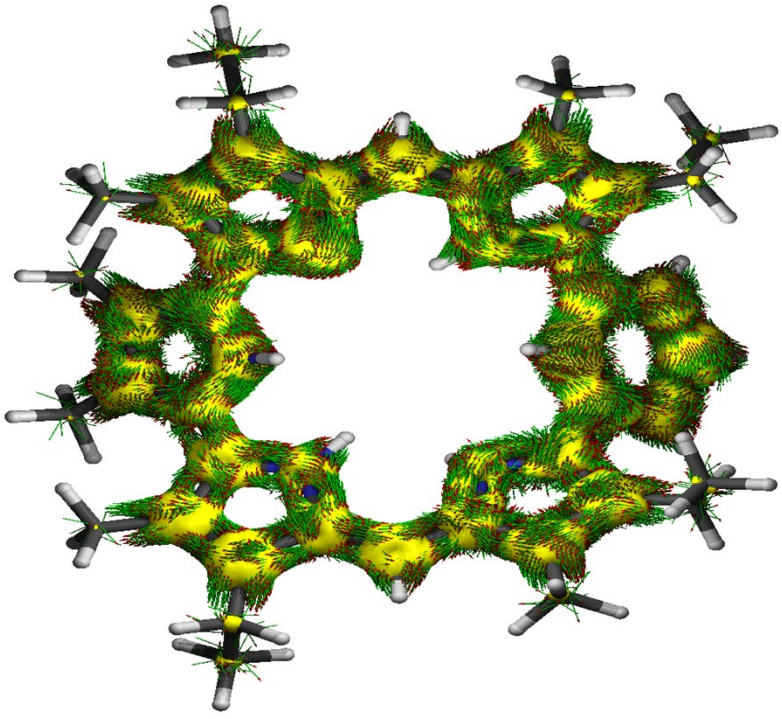

Figure S16. Calculated anisotropy induced current density (ACID) plot of diprotonated pyriamethyrin **1b**. Current density vectors indicate a strong paratropic global current.

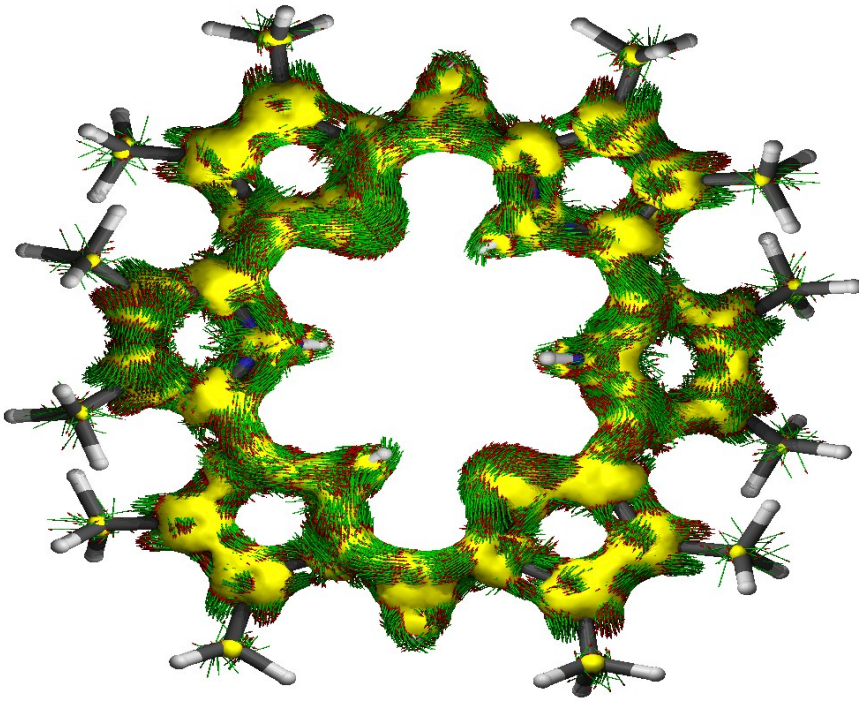

Figure S17. Calculated anisotropy induced current density (ACID) plot of amethyrin **2**. Current density vectors indicate a strong paratropic global current.

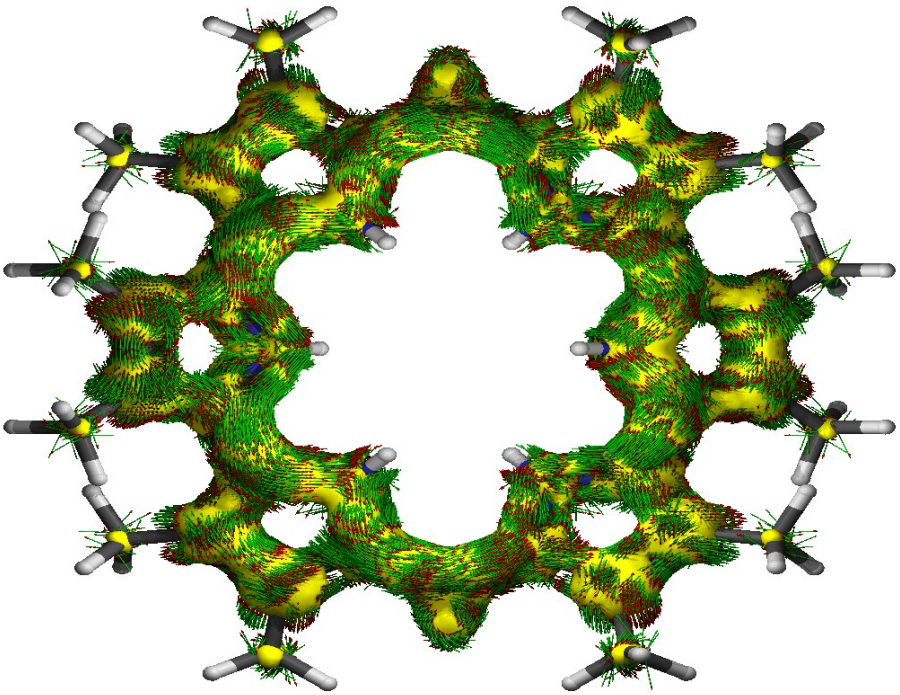

Figure S18. Calculated anisotropy induced current density (ACID) plot of diprotonated amethyrin **2b**. Current density vectors indicate a strong paratropic global current.

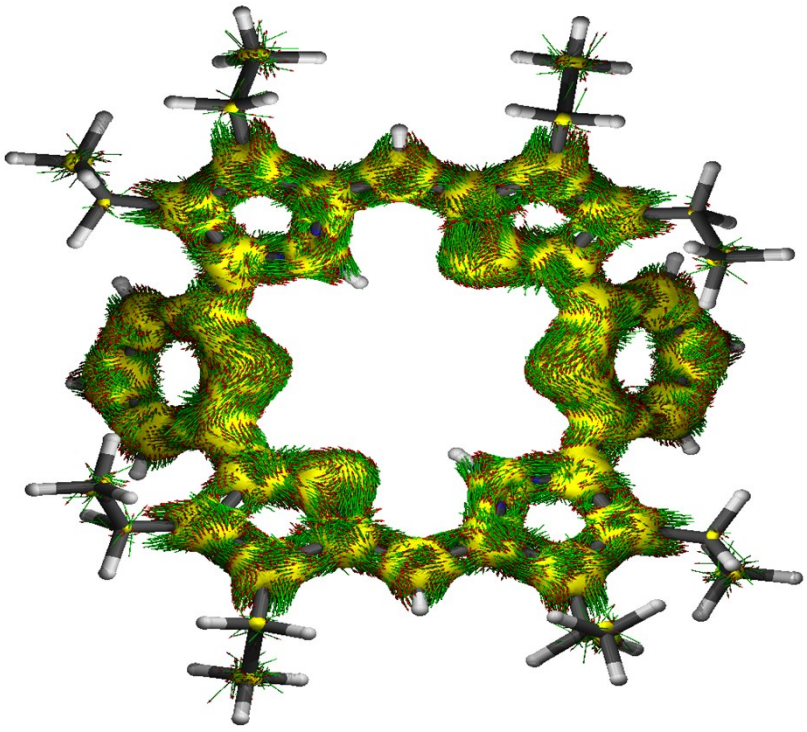

Figure S19. Calculated anisotropy induced current density (ACID) plot of dipyriamethyrin **3**. Current density vectors indicate little global current directionality

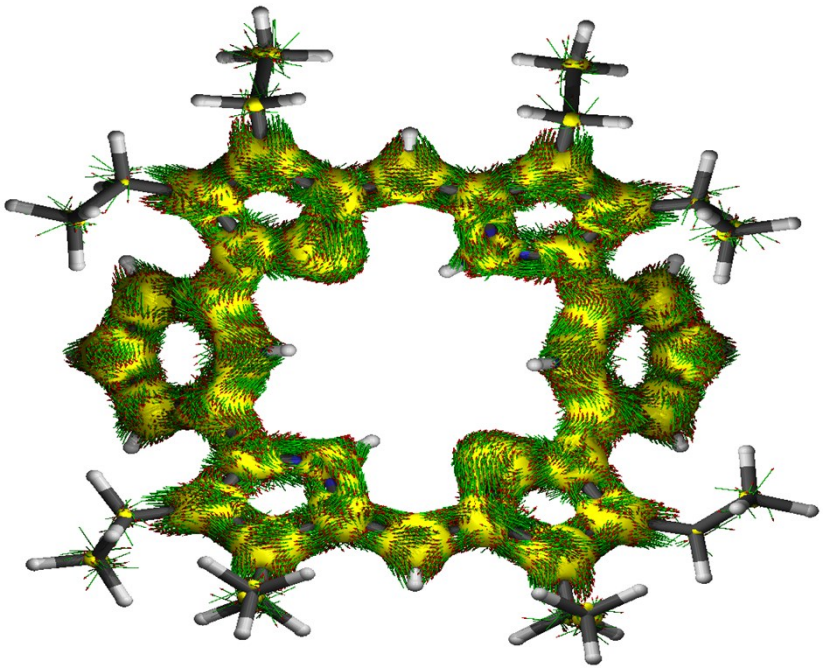

Figure S20. Calculated anisotropy induced current density (ACID) plot of diprotonated dipyriamethyrin **3b**. Current density vectors indicate a strong paratropic global current.

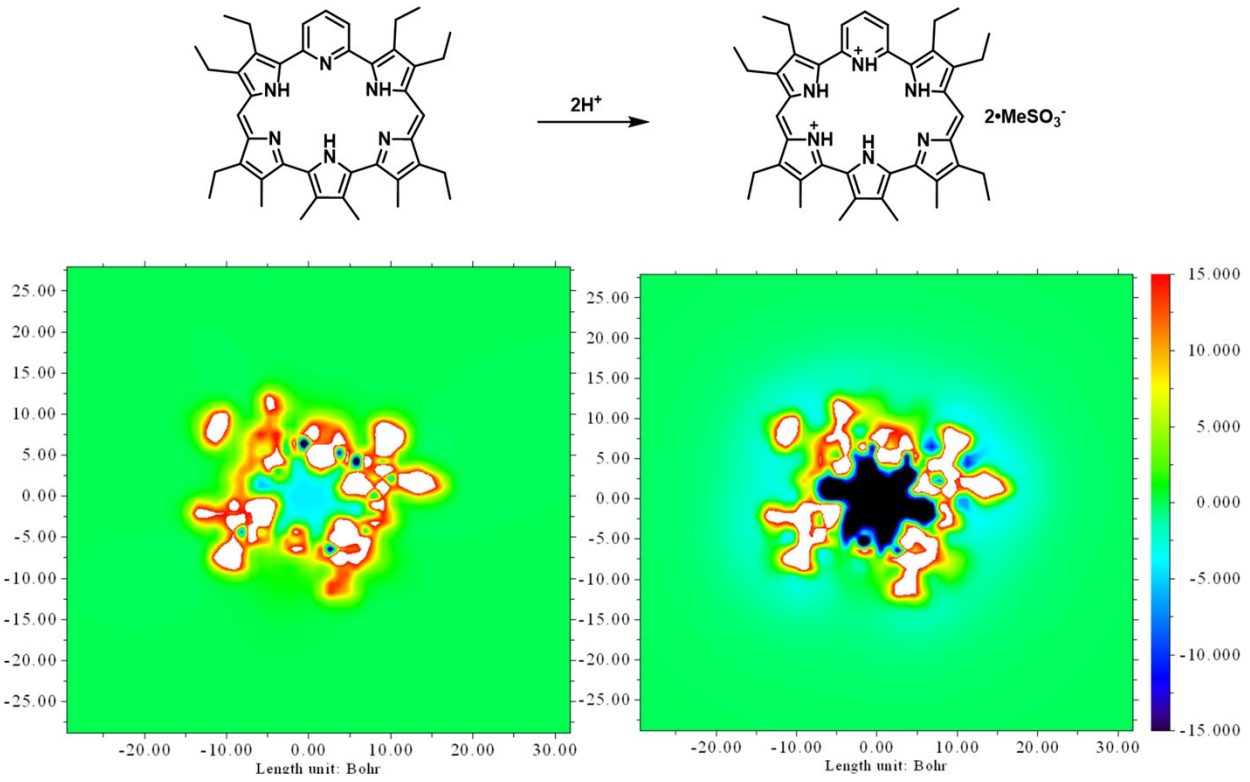

Figure S21. Calculated iso-chemical surface shielding (ICSS) for neutral and diprotonated pyriamethyrin (**1** and **1b**).

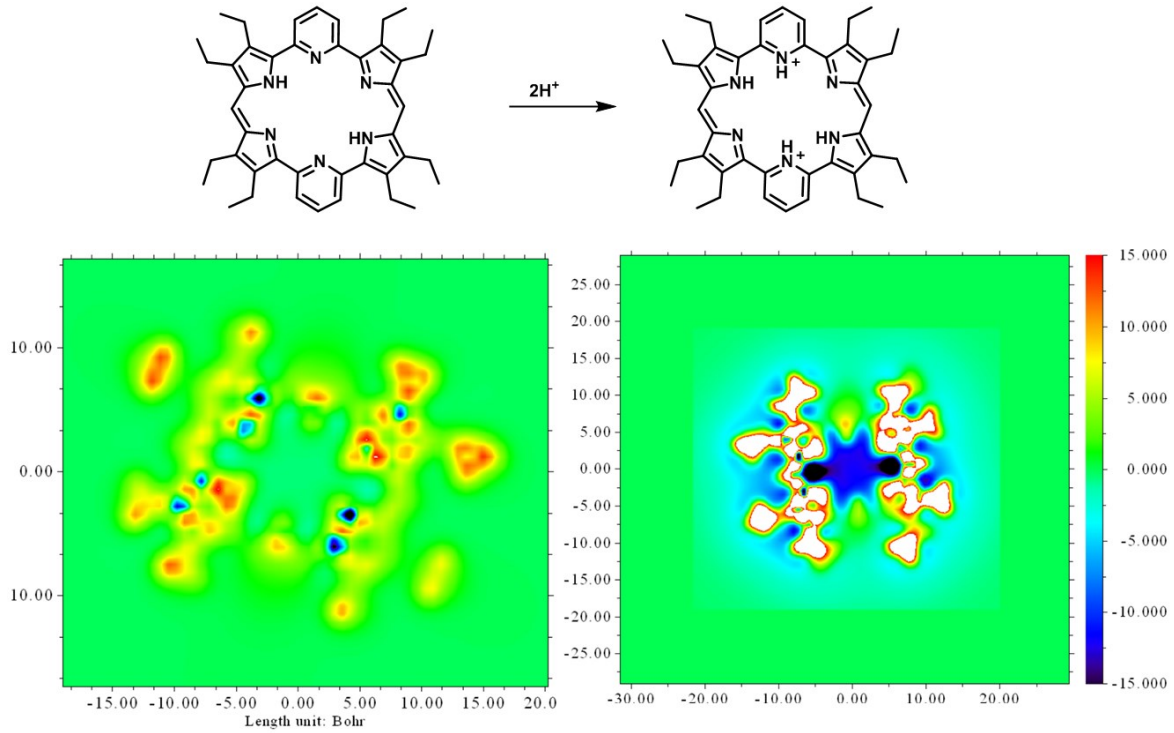

Figure S22. Calculated iso-chemical surface shielding (ICSS) for neutral and diprotonated pyriamethyrin (**3** and **3b**).

References

1 J. L. Sessler, S. J. Weghorn, Y. Hiseada and V. Lynch, *Chem. – A Eur. J.*, 1995, **1**, 56–67.

2 J. T. Brewster, Q. He, G. Anguera, M. D. Moore, X. S. Ke, V. M. Lynch and J. L. Sessler, *Chem. Commun.*, 2017, **53**, 4981–4984.

3 J. T. Brewster, H. D. Root, D. Mangel, A. Samia, H. Zafar, A. C. Sedgwick, V. M. Lynch and J. L. Sessler, *Chem. Sci.*, 2019, 5596–5602.

4 R. Valiev, H. Fliegl, and D. Sundholm, *Chem. Commun.*, 2017, **53** , 9866 —9869.

5 T. M. Krygowski, M. K. Cyrański, *Chem. Rev.* 2001, **101**, 5, 1385–1420.